A TURBULENCE MODEL FOR ACCELERATION OF THE HIGH LATITUDE FAST SOLAR WIND

Verdini A.[1], **Dmitruk P.**[2], **Matthaeus W. H.**[2], **Oughton S.**[3], **and Velli M.**[1]

[1] *Dipartimento di Astronomia e Scienza dello Spazio, Firenze, Italy*
[2] *Bartol Research Institute, University of Delaware, Newark, Delaware 19716, USA*
[3] *Department of Mathematics, University of Waikato, Private Bag 3105, Hamilton, New Zeland*

ABSTRACT

Observations such as Spartan and SOHO UVCS have challenged ideas for the acceleration of the solar wind by constraining models to produce > 1.5 Million K protons, several hundred km s^{-1} radial outflows, and > 700 km s^{-1} terminal speeds in the wind emanating from polar coronal holes, with coronal electrons remaining cooler than protons. Observed properties of the solar wind at 1AU and by Ulysses provide additional constraints on these models. It was recognized some time ago (e.g. Habbal et al., 1995; McKenzie et al., 1995) that these conditions probably require adding internal energy in sufficient quantities at altitudes $< 1.5\ R_\odot$, but the origin of this energy and its method of transport and conversion to heat have remained unclear. The involvement of turbulence in this process was suggested some time ago (Coleman, 1968; Hollweg, 1986; Matthaeus et al., 1999), but various issues regarding the physics of cascade and dissipation have persisted (e.g. Matthaeus et al., 2003) and a wind model compatible with magnetohydrodynamic theories of turbulence, including the physics of low frequency anisotropic cascade, has not yet been presented to our knowledge. Here we suggest some simplifications and assumptions that allow a self-consistent semi-analytical treatment of the solar wind acceleration problem.

Key words: Waves; Turbulence; Solar Wind.

1. MODEL EQUATIONS AND ASSUMPTION

Combining a simple turbulence closure model (Dmitruk et al., 2001) with a one-dimensional model of a coronal hole, we solve the continuity equation, momentum equation with ponderomotive force due to turbulence, an internal energy equation with turbulent dissipation, and the turbulence closure equations for upward- and downward-propagating low frequency turbulence amplitudes. The the large scale density, velocity and (total) pressure equations (hereafter referred as wind equations) are:

$$\frac{d}{dr}\left[\rho U A\right] = 0, \tag{1}$$

$$\rho U \frac{dU}{dr} = -\nabla P' - \rho \frac{GM_{\rm sun}}{r^2} + \left\langle \frac{\delta\mathbf{B}\cdot\boldsymbol{\nabla}\delta\mathbf{B}}{4\pi} - \rho\delta\mathbf{u}\cdot\boldsymbol{\nabla}\delta\mathbf{u} \right\rangle, \tag{2}$$

$$U\frac{dp}{dr} = -\gamma p \nabla\cdot\mathbf{U} + (\gamma-1)Q(r), \tag{3}$$

where

$$P' = 2nk_{\rm B}T + \frac{b^2}{2} \equiv p + \frac{b^2}{2}.$$

Notably we assume that for the turbulence decay rate the heating function $Q(r)$ has the form:

$$\frac{Q(r)}{\rho} = \frac{Z_- Z_+^2 + Z_+ Z_-^2}{2\lambda}. \tag{4}$$

We specify the area expansion factor $A(r)$, and use conservation of magnetic flux, $B_r(r)A(r) = B_r A|_{1\,AU} = const$, employing observational constraints and impose $\lambda = \lambda_0\sqrt{A(r)}$. Note also that we include the Reynods stress in the momentum equation, that is the last term in eq. 2. The dissipation, the magnetic pressure and the ponderomotive forces depend upon the small-scale fields, explicitly recast in term of the Elsässer variables, $Z_\pm$, in the energy equation. These are incompressible, transverse fluctuations of the magnetic and velocity field propagating downward and upward, respectively, along the mean magnetic field lines. For a given profile of the radial wind speed and Alfvén speed one can integrate the wave equations (hereafter referred as "wave" equations), which in stationary form are:

$$\left[U \mp V_A(r)\right]\frac{dz_\pm}{dr} = +i\omega z_\pm \pm R_1 z_\mp \mp R_2 z_\pm - \frac{|Z_\mp|}{2\lambda} z_\pm. \tag{5}$$

The reflection coefficients are given by the large-scale gradients,

$$R_1 = \frac{1}{2}\frac{dV_A}{dr} \pm \frac{1}{4}\frac{dU}{dr} \mp \frac{1}{4}U\frac{dlogA}{dr}, \tag{6}$$

Proc. SOHO 17 – 10 Years of SOHO and Beyond, Giardini Naxos, Sicily, Italy
7 – 12 May 2006 (ESA SP-617, July 2006)

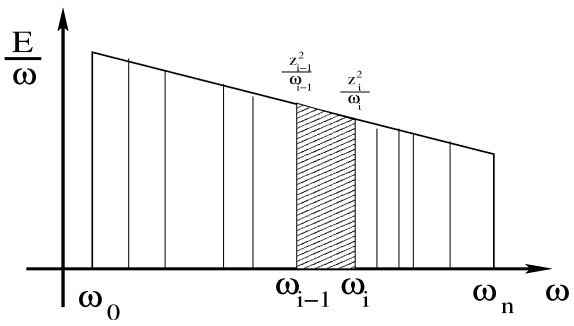

Figure 1. Frequency integrated amplitudes

$$R_2 = \frac{1}{2}\frac{dV_A}{dr} + \frac{1}{2}V_A\frac{dlogA}{dr} \pm \frac{1}{4}\frac{dU}{dr} \pm \frac{1}{4}U\frac{dlogA}{dr}. \quad (7)$$

Here $V_A = V_{A_r}(r) = B_r/\sqrt{4\pi\rho}$, $U = U_r(r)$ and $A = 1/B_r$ is the area (expansion) factor (for example $A = r^2$ for a radially symmetric case).

It is assumed that the parallel gradients are much weaker than the transverse ones and that the $z_\pm$ acts as surrogates of the frequency decomposition of the full amplitudes $Z_\pm$, allowed by the stationarity of the "wind" equations. In effect, it is assumed that

$$\langle z_\pm^2 \rangle \equiv Z_\pm^2 = \frac{1}{2}\sum_1^n \left(\frac{{z_i}_\pm^2}{\omega_i} + \frac{{z_{i-1}}_\pm^2}{\omega_{i-1}} \right)(\omega_i - \omega_{i-1}), \quad (8)$$

with reference to fig. 1. Note that the nonlinear interactions occur with the frequency integrated fields $Z_\pm$ and that the magnetic pressure and the ponderomotive force are computed using these integrated quantities as well.
(See Hossain et al., 1995; Dobrowolny et al., 1980; Grappin et al., 1982 for background on this one point closure.)

The procedure for the integration follows a scheme similar to that one used by MacGregor and Charbonneau (1994). We start with an imposed temperature profile and $\gamma = 1$. Solve the wind equations (1-2) starting at 1 $R_\odot$ with the wave-derived quantities (ponderomotive force, magnetic pressure and dissipation) set to zero. Boundary conditions for the "wave" equations are naturally imposed at the Alfvénic critical point (x_a). With the wind and Alfvén speed found in the previous integration, equations (5) are integrated backward in order to find the wave amplitude to impose at x_a which corresponds to a given reference velocity field fluctuation amplitude at the base (say $\delta u = 25$ km s^{-1}). Then the waves are integrated forward until 1 AU. After the first step Eqs. (1-3) are integrated simultaneously with $\gamma_{iter} = \gamma_{iter-1} + \epsilon_\gamma$, and the contribution of the wave-derived quantities are included, to get the wind and Alfvén speed profile, which are then used again in the waves equations, and so on. When $\gamma = 5/3$ is achieved, the integration continues until convergence is reached, that is, when the relative variation of the quantities U, V_a, T, Q/ρ, xa, xs is less than 0.01% (Here, xs is the sonic critical point).

2. PRELIMINARY RESULTS

We present here some preliminary result of runs which are not converged to the value $\gamma = 5/3$ due to some spurious numerical effects which propagate through the iterative scheme we are using. Two cases are considered which differ only for the frequencies used in the wave equations. In figure 2 the resulting profile of the wind speed, temperature, turbulence level, the normalized cross helicity and density are shown for $\gamma = 1.4$, using the following definitions:

$$\text{Turbulence level } = E^+ + E^- = \frac{1}{2}(Z_+^2 + Z_-^2),$$

$$\text{Normalized cross helicity } \equiv \sigma_c = \frac{Z_+^2 - Z_-^2}{Z_+^2 + Z_-^2}.$$

Dashed lines refer to the case in which only one frequency is used to describe the small scale fields, namely a zero frequency (an approximation valid for frequencies up to 10^{-5} Hz because of their common reflection rate). Solid lines refer to the case in which a flat spectrum is imposed at x_a with frequencies in the interval 10^{-5} Hz $< \nu < 10^{-3}$ Hz (8 waves are used to describe the spectrum) so that also relatively high frequencies are included (the ones usually described by a WKB approximation). In the plots are also shown some observational constraints, namely: (McComas et al., 2000) for the wind speed and density at 1 AU, (Grall et al., 1996) for the wind speed inside 1 AU, (Breech et al., 2005) for the normalized cross helicity and temperature beyond 1 AU, (Kohl et al., 1995) for the temperature inside 1 AU, (Banerjee et al., 1998; Fisher and Guhathakurta, 1995) for the density inside 1 AU, (Matthaeus et al., 2004) for the turbulence level. The ripple in the wind speed is due to the unusual minimum of temperature found around 3 $R_\odot$ which is a combined effect of the adiabatic cooling and the reduction of the dissipation close to the minimum of the reflection rate. It is the dissipation itself which causes the reduction of the backward propagating Alfvén waves (the disappearance for the single frequency case) and hence limits its contribution close to the sun. However, wind speed and turbulence level plots shows a good trend compared to the data, despite density is an order of magnitude lower and the temperature profile close to the sun and the cross helicity are remarkably wrong. Note that the number of wave considered and overall their frequency change substantially the solution, since they directly influence the efficiency of the dissipation (Verdini et al., 2005).

3. CONCLUSIONS

A turbulence model of the type we propose here has promise to explain the Solar Wind acceleration without appeal to artificial heat dissipation, equation of state or further damp mechanism. At present some observational constraints are not well reproduce, and we believe that better results will be found when the present numerical difficulties are solved. There are good indications from the wind speed profile, encouraging us to continue in this path. There are many parameters which can be varied such as the overexpansion factors of the flux tube, the base amplitude of the velocity field fluctuations, the frequency considered and the spectrum slope imposed at the Alfvénic critical point, which can substantially change the profile shown (especially for the temperature).

REFERENCES

Banerjee, D., Teriaca, L., Doyle, J. G., and Wilhelm, K., 1998, Astron. Astrophys. **339**, 208

Breech, B., Matthaeus, W. H., Minnie, J., Oughton, S., Parhi, S., Bieber, J. W., and Bavassano, B., 2005, Geophys. Rev. Lett. **32**, 6103

Coleman, P. J., 1968, Astrophys. J. **153**, 371

Dmitruk, P., Milano, L. J., and Matthaeus, W. H., 2001, Astrophys. J. **548**, 482

Dobrowolny, M., Mangeney, A., and Veltri, P., 1980, Phys. Rev. Lett. **45**, 144

Fisher, R. and Guhathakurta, M., 1995, ApJ Lett. **447**, L139+

Grall, R. R., Coles, W. A., Klinglesmith, M. T., Breen, A. R., Williams, P. J. S., Markkanen, J., and Esser, R., 1996, Nat **379**, 429

Grappin, R., Frisch, U., Léorat, J., and Pouquet, A., 1982, Astron. Astrophys. **105**, 6

Habbal, S. R., Esser, R., Guhathakurta, M., and Fisher, R. R., 1995, Geophys. Rev. Lett. **22**, 1465

Hollweg, J. V., 1986, J. Geophys. Res. **91**, 4111

Hossain, M., Gray, P. C., Pontius Jr., D. H., Matthaeus, W. H., and Oughton, S., 1995, Phys. Fluids **7**, 2886

Kohl, J. L. et al., 1995, Space Sci. Rev. **72**, 29

MacGregor, K. B. and Charbonneau, P., 1994, Astrophys. J. **430**, 387

Matthaeus, W. H., Minnie, J., Breech, B., Parhi, S., Bieber, J. W., and Oughton, S., 2004, Geophys. Rev. Lett. **31**, 12803

Matthaeus, W. H., Mullan, D. J., Dmitruk, P., Milano, L., and Oughton, S., 2003, Nonlin. Process. Geophys. **10**, 93

Matthaeus, W. H., Zank, G. P., Oughton, S., Mullan, D. J., and Dmitruk, P., 1999, Astrophys. J. **523**, L93

McComas, D. J., Barraclough, B. L., Funsten, H. O., Gosling, J. T., Santiago-Muñoz, E., Skoug, R. M., Goldstein, B. E., Neugebauer, M., Riley, P., and Balogh, A., 2000, J. Geophys. Res. **105**, 10419

McKenzie, J. F., Banaszkiewicz, M., and Axford, W. I., 1995, Astron. Astrophys. **303**, L45

Verdini, A., Velli, M., and Oughton, S., 2005, Astron. Astrophys. **444**, 233

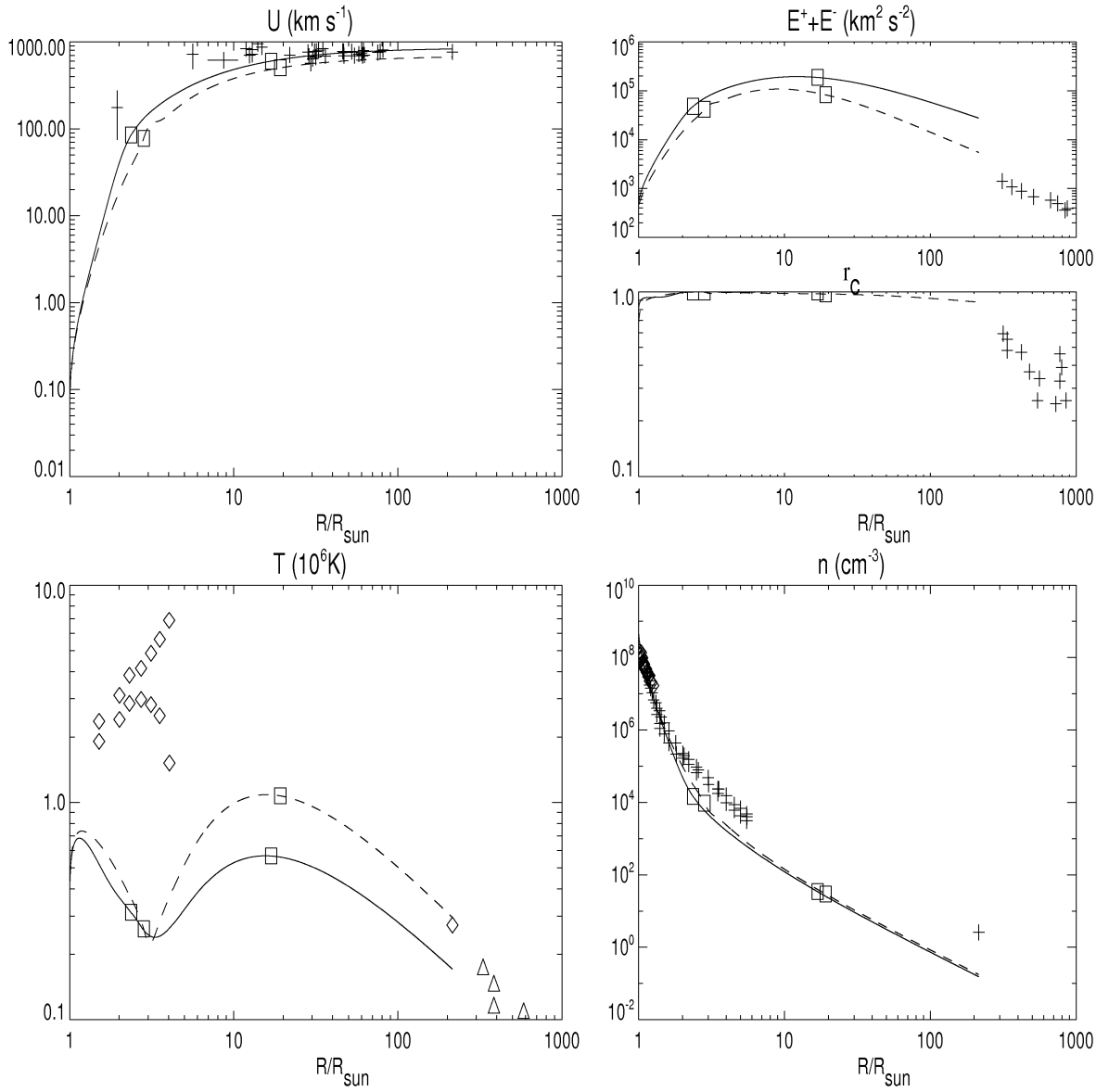

Figure 2. Wind speed, turbulence level, normalized cross helicity, temperature and density for the single frequency (dashed lines) and multi-frequency (solid line) case at $\gamma = 1.4$. The squares mark the sonic and Alfvénic critical points (inner and outer squares respectively). Other symbols indicate observational constraints, see text for references